frontiers | Frontiers in Earth Science

# Geophysical evidence for submarine methane seepage on the Western slope of Okinawa Trough

Di Luo[1,2], Feng Cai[1,2]*, Qing Li[1,2], Guijing Yan[1,2], Yunbao Sun[1,2], Ang Li[1,2] and Gang Dong[1,2]

[1]Key Laboratory of Marine Hydrocarbon Resources and Environmental Geology, Ministry of Land and Resources, Qingdao Institute of Marine Geology, Qingdao, China, [2]Laboratory for Marine Mineral Resources, Qingdao National Laboratory for Marine Science and Technology, Qingdao, China

Identifying seafloor methane seepage efficiently has important implications for assessing environmental impact, reducing the uncertainty of top seal integrity, understanding the petroleum system, and mitigating the drilling hazards due to shallow gas influx. Pore water geochemistry analyses suggest that the study area has an extremely high methane seepage flux and active methane anaerobic oxidation processes. However, geochemical data cannot provide details about the internal seepages. The geophysical dataset from the Western slope of Okinawa Trough, including 2D high-resolution seismic, sub-bottom profiles, and bathymetry, gives us a good opportunity to understand the detailed characteristics of methane seepages in this study. Geophysical data have revealed numerous methane seepage-related features such as seismic chimneys, pockmarks, submarine domes, and amplitude anomalies, including bright spots and enhanced reflections. Pockmarks and domes are often associated with seismic chimneys, indicating that fluid migration is important in their formation. The various geophysical expressions may represent different stages of methane seepage. Fluid quickly drains, causing severe sediment deformation and forming pockmarks, whereas domes may indicate the early stages of fluid discharge. Chimneys that do not extend to the seafloor may indicate that the venting is gradual and focused. Flares linked to domes or pockmarks may indicate that the fluid migration is active. Several factors triggered the existence of methane seepages on the Western slope of the Okinawa Trough, including tectonic setting, overpressure and rapid sedimentation.
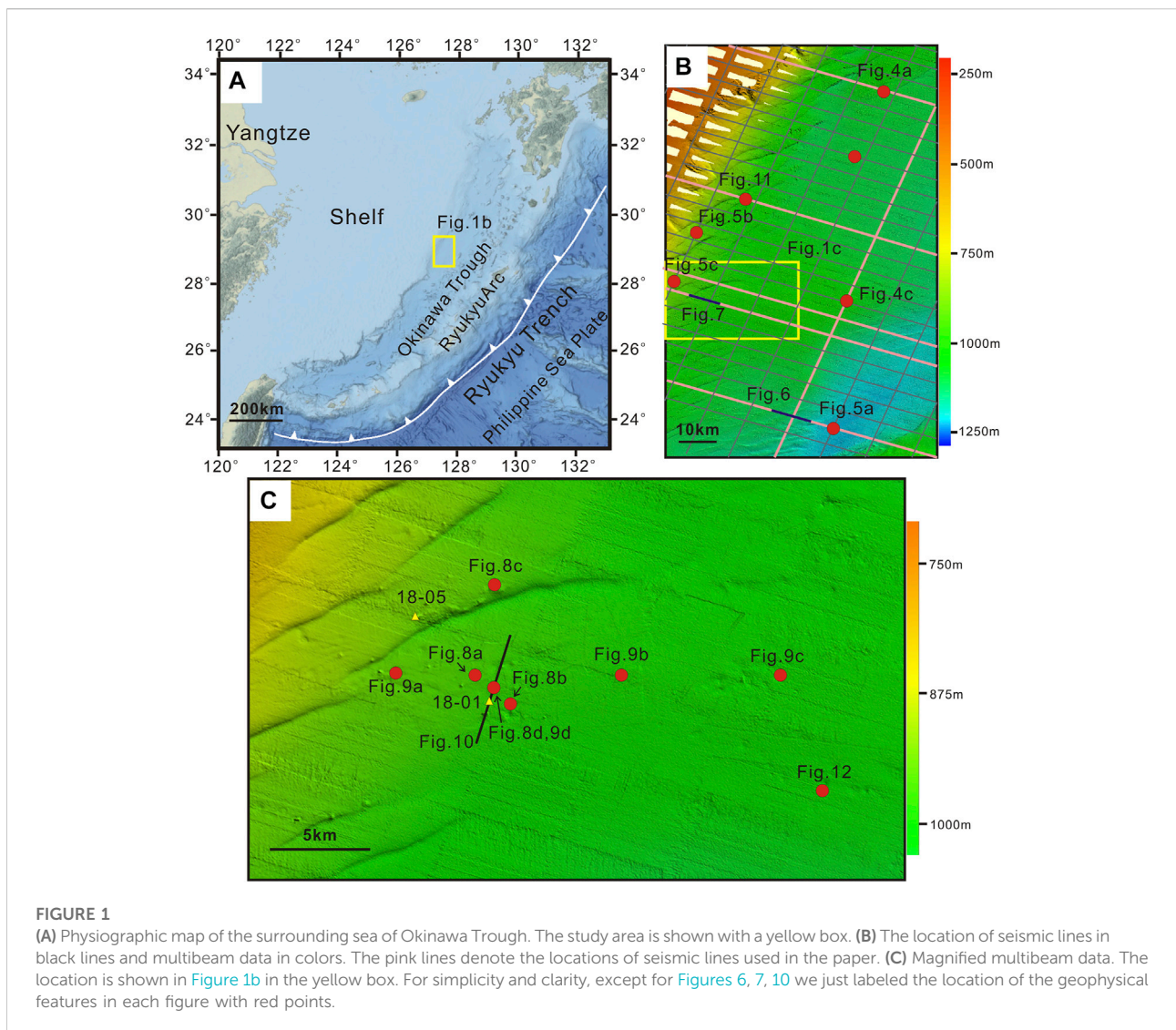
## Introduction

Submarine methane seepage is a geological phenomenon widespread on both active (Netzeband et al., 2010; Tsunogai et al., 2012; Crutchley et al., 2013; Wei et al., 2021) and passive continental margins (Miller et al., 2012; Wenau et al., 2015; Dewangan et al., 2021). Since the discovery of methane seepage into the modern marine environment at the foot of the Florida Escarpment (Paull et al., 1984), the seepage of methane-rich fluids from sediments into the ocean floor or atmosphere has been revealed to be a common feature along continental margins (Williscroft et al., 2017).

Methane seepage has a significant impact on global climate change, the global carbon cycle, ocean acidification, and the chemosynthetic ecosystem (Wei, et al., 2021). Methane is abundant as free bubbles, aqueous methane, and/or gas hydrates in continental margin sediments and is an important component of the global carbon cycle (Suess, 2014; Xu et al., 2021). Their escape

from marine sediments could cause oceanic acidification and deoxygenation, as well as amplify climatic warming if they enter the atmosphere (Li et al., 2021). Moreover, several authors have discussed a relationship between methane seepage and gas hydrate reservoirs, such as the Krishna-Godavari offshore basin (Gullapalli et al., 2019), Black Sea (Shnyukov, 2013), offshore western Svalbard (Graves et al., 2017), Taixinan basin (Wang et al., 2018), Hikurangi Margin (Schwalenberg et al., 2010; Krabbenhoeft et al., 2013). Methane in marine sediments is produced by microbial and thermal degradation of organic carbon. If sediment pore fluids become methane saturated and temperature is low while the pressure is relatively high (Graves, et al., 2017), gas hydrate may form. On the other hand, gas hydrate decomposition is an important source of methane (Van Rensbergen et al., 2002). Warming bottom waters have begun to dissociate large amounts of gas hydrate and the resulting methane release may accelerate global warming (Berndt et al., 2014).



**FIGURE 1**
**(A)** Physiographic map of the surrounding sea of Okinawa Trough. The study area is shown with a yellow box. **(B)** The location of seismic lines in black lines and multibeam data in colors. The pink lines denote the locations of seismic lines used in the paper. **(C)** Magnified multibeam data. The location is shown in Figure 1b in the yellow box. For simplicity and clarity, except for Figures 6, 7, 10 we just labeled the location of the geophysical features in each figure with red points.
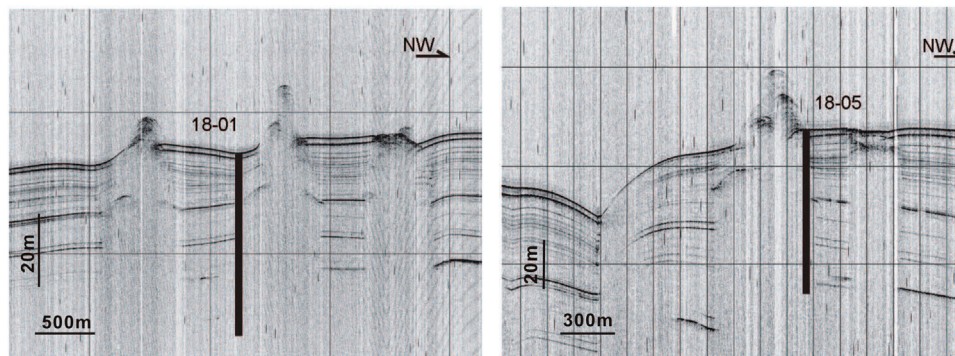
**FIGURE 2**
Sub-bottom profiles across two drilling sites.

As mentioned above, efficiently detecting and identifying seafloor methane seepage has significant implications (Dixit and Mandal, 2020). Geochemical analysis of pore water or bottom water (Xu et al., 2018), synthetic aperture radar (SAR) (Logan et al., 2010), and seafloor observations such as Remotely Operated Vehicle (Palomino et al., 2016) are conventional practices for detecting methane seepage. However, because of inadequate sampling density and limited investigation depth, these techniques are low-efficiency and only provide shallow-depth information about fluid migration pathways. The seepage and expulsion of methane-rich fluids can create various geological features (Netzeband, et al., 2010). Topographic expressions at the seafloor range from build-ups (e.g. mud volcanoes (Milkov, 2000; Tsunogai, et al., 2012; Magalhaes et al., 2019), mounds [Chun et al., 2011; Somoza et al., 2014; Benjamin and Huuse, 2017) or domes (Koch et al., 2015)] to depressions [e.g., submarine pockmarks (Cathles et al., 2010; Dondurur et al., 2011; Callow et al., 2021)]. Furthermore, many studies revealed that fluid migration pathways were associated with buried underlying structures such as mud diapirs (Rovere et al., 2014; He et al., 2016; Wan et al., 2017), fault systems (Mohammedyasin et al., 2016; Hillman et al., 2020), and seismic chimneys (Kempka et al., 2016; Callow, et al., 2021).

The Okinawa Trough is an active back-arc basin formed by the subduction of the Philippine Sea Plate beneath the Eurasian Plate to the northwest (Figure 1A). Several geological indicators of methane seepage such as abundant authigenic carbonates (Guan et al., 2019; Wang et al., 2019; Guan et al., 2022), concretions, and chimneys (Sun et al., 2015; Xu, et al., 2021) have been discovered along the western slope of the Okinawa Trough. In addition, some mud diapirs (Ning et al., 2009; Xing et al., 2016), and mud volcanoes (Yin et al., 2003) accompanied by fluid flows have been identified from seismic

and bathymetric data in the middle and southern sections of the Okinawa Trough. Geochemical data from the pore water of the gravity cores reveals active methane seepage in the vicinity of mud volcanoes (Li et al., 2015; Xu et al., 2018; Xu et al., 2021). In this study, we systematically demonstrate the geophysical properties of methane seepages from the western slope of the Okinawa Trough using high-resolution seismic reflection data (Figure 1B), parametric sub-bottom profiles, and multibeam bathymetric (Figure 1C). A variety of geophysical anomalies associated with methane seepages are interpreted and illustrated.

## Geological background

The Okinawa Trough, which extends from the Ilan Plain in northeastern Taiwan to the shallow sea southwest of Kyushu (Sibuet et al., 1987), is an active back-arc basin formed by the subduction of the Philippine Sea Plate beneath the Eurasian Plate to the northwest (Figure 1) (Sibuet et al., 1998). It is divided into northern, middle, and southern segments that are separated by the Tokara Fault and the Miyako Fault zones (Sibuet, et al., 1987). The stages of back-arc evolution in the three segments are very different. The northern Okinawa Trough is experiencing crustal stretching, the middle Okinawa Trough is undergoing propagating rift processes, and the southern Okinawa Trough presents signs of initial ocean crust spreading. The stages of back-arc evolution in the Okinawa Trough vary from continental extension in the northern Okinawa Trough, rifting in the middle Okinawa Trough, and potential seafloor spreading in the southern Okinawa Trough. It is considered to be in the rifting phase prior to the back-arc spreading (Park et al., 1998), and has complex geotectonic features. Along the axis of the middle to southern Okinawa
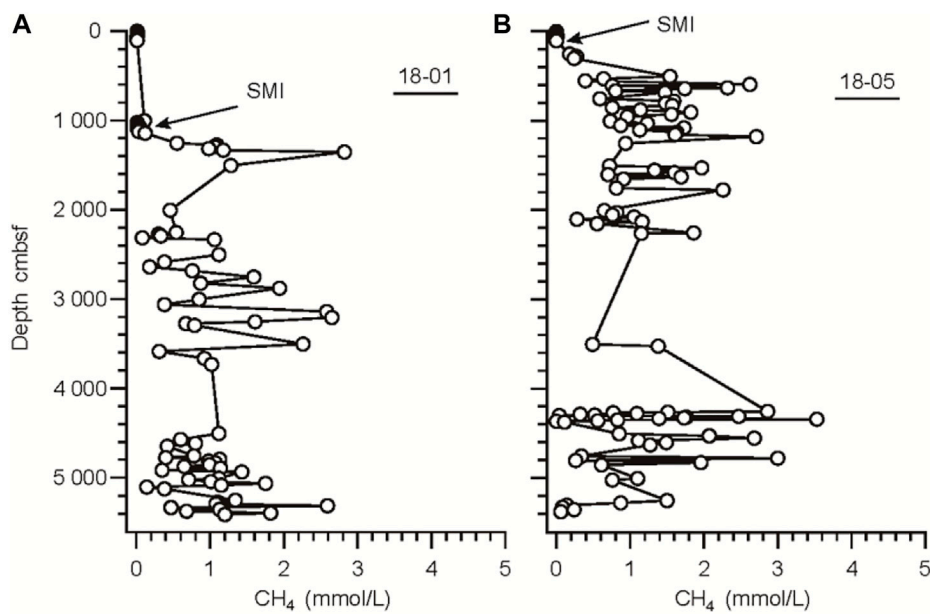
**FIGURE 3**
Depth profiles of headspace methane concentration in pore water of 18-01 **(A)** and **(B)** 18-05 sites.

Trough, several en-echelon extensional grabens with active faults have been identified (Shinjo and Kato, 2000).

The width of the Okinawa Trough increases from 60 to 100 km in the south to 230 km in the north, while the water depth decreases from 2,300 m to 200 m from south to north (Sibuet et al., 1987; Sibuet et al., 1998; Tsai et al., 2021). The crust and sedimentary layers become gradually thinner along the length of the trough, from 20 to 30 km in the north to 10–12 km in the south (Minami et al., 2022). The northern Okinawa Trough is composed of numerous half-grabens covered by thick terrigenous material layers up to 8 km thick from China's Yangtze and Yellow rivers, whereas the southern Okinawa Trough has a sedimentary cover of up to 2 km. The middle Okinawa Trough has received varying sedimentary supplies from those rivers, and the sedimentary rate has increased considerably over the last 0.5 million years (Sibuet, et al., 1987).

Heat flows in the Okinawa Trough are high ($10^2$–$10^5$ mW/m2), which may be caused by present or recent hydrothermal activities associated with the rifting process, according to heat flow studies (Chen et al., 2020). In the southernmost Okinawa Trough, several submarine volcanoes emitting intense gas plumes from the seafloor have been discovered (Tsai, et al., 2021). The geochemical data from pore water on the Western slope of the Okinawa Trough reveals methane seepage in the turbidite deposits is active (Li, et al., 2015) Figure 1b.

# Data and methods

## Small-scale and high-resolution multichannel seismic

Small-scale and high-resolution marine multichannel seismic detection technology using large energy sparkers seismic source is characterized by a high dominant frequency, wide bandwidth, and high resolution. When compared with traditional method, this technology has the advantages of high resolution (the vertical resolution is up to 1–3 m) and high detection precision (Luo et al., 2017). The high-resolution multichannel seismic data used in this study were acquired using a SIG pulse L5 Sparker with a shooting energy of 20 kJ at every 12.5 m, a 293.75 m streamer (48 channel, 6.25 m group interval) and 12 times stacking fold. The shortest source-receiver distance was 75 m with recording length of 4,000 ms. The data was sampled at an interval of 0.5 ms. Based on the characteristics of the seismic detection technology, targeted processing technologies were applied to improve the quality of seismic data imaging (Luo et al., 2019). Parametric sub-bottom profiles.

The parametric sub-bottom profiles survey is a geophysical method based on acoustic theory to detect shallow formations and structures beneath the seafloor and is one of the important means of marine geological survey. It is useful for identifying the acoustic anomalies of marine sediments.
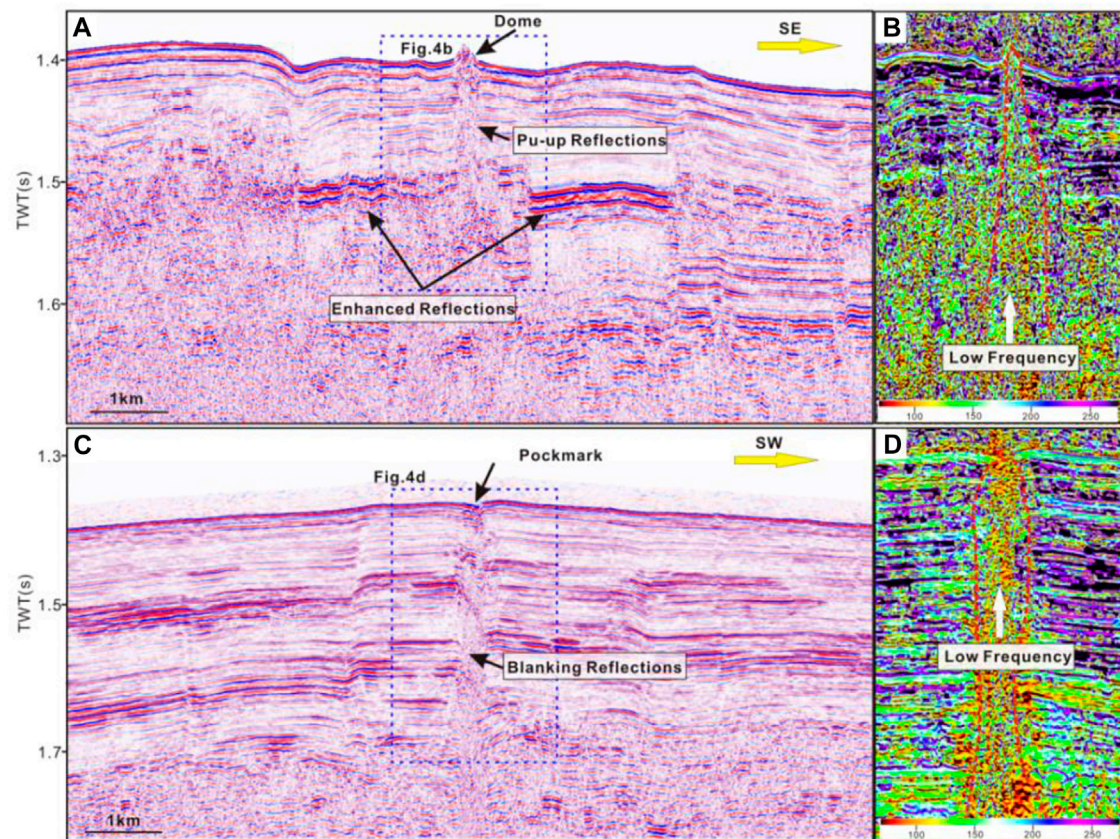
**FIGURE 4**
Type-A seismic chimneys. **(A,C)** Seismic profiles. A dome or pockmark is observed above chimneys; **(B,D)** The instantaneous frequency attribute profiles, which locations are shown in Figure 4A. Low-frequency anomalies are observed within the chimneys. See locations in Figure 1B.

Sub-bottom profile data used in the study were acquired with the TOPAS PS18 system, with a primary frequency ranging from 2 to 6 kHz. The chirp (Compressed High-Intensity Radar Pulse) technique, which has high penetration, was used for the source pulse. The sound speed of the transducer is 1,500 m/s.
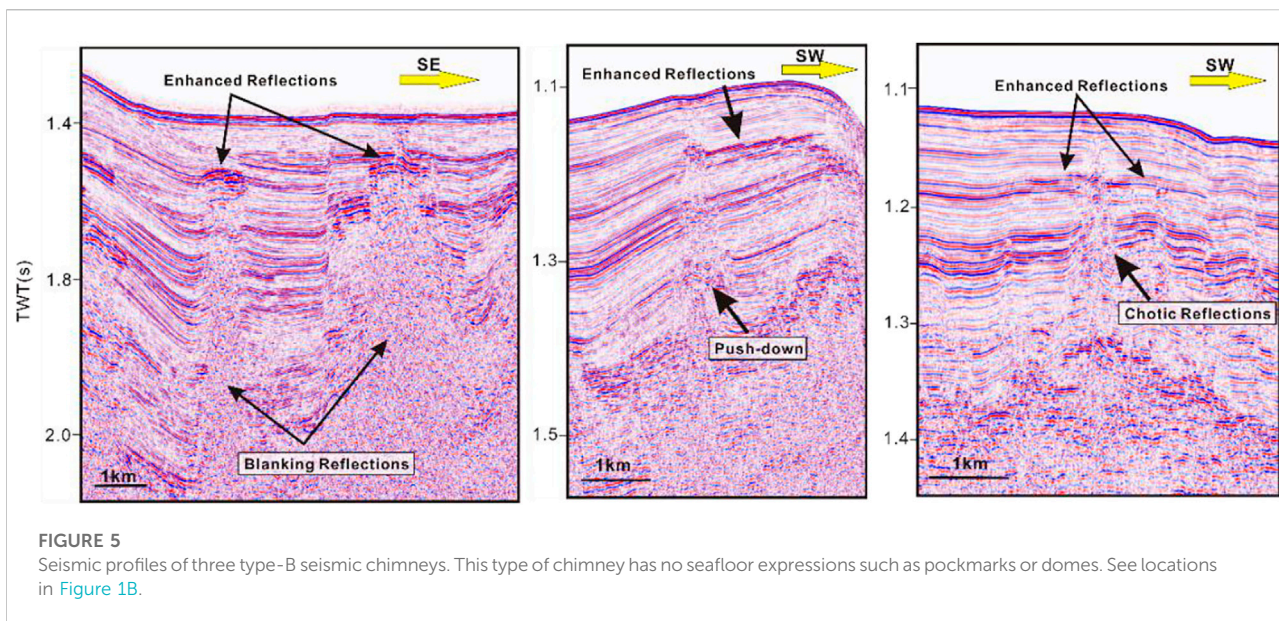
## Multibeam bathymetric

The bathymetric data present in this paper was acquired using a Kongsberg Simrad EM122 multi beam echo sounder system. It has a swath angle of 130 and can transmit and receive up to 288 simultaneous beams with a beamwidth of 1 by 1. The sounding frequency of the system is 12 kHz and up to 864 soundings per ping in the dual-swath mode. The data has been processed using QPS Qimera software.

## Sediment pore water sampling

The sediment samples for this study were obtained using the seabed drilling rig, with a drilling capacity of 60 m at a water depth of 3,500 m.

According to geophysics data, several mud volcanoes or domes formed on the western slope of the Okinawa Trough, and both boreholes (18-1 and 18-5) are located on the flanks of the mud volcanoes (Figure 2) (Li et al., 2020). The distance between borehole 18-01 and the mud volcano is about 10 m, and borehole 18-05 is located next to the mud volcano.

Pore water was squeezed by pressure filtration, and the sampling interval was 20 cm. Each core section was split into two halves for geochemical analysis and archiving. About 5 cm of thick sediment is used for pore water squeezing. Part of the pore water is used for onboard sulfate, chloride ion, hydrogen sulfide, nutrients ($NH_4^+$, $NO_3^-$, $NO_2^-$, $PO_4^{3-}$, $SiO_2$), and total

**FIGURE 5**
Seismic profiles of three type-B seismic chimneys. This type of chimney has no seafloor expressions such as pockmarks or domes. See locations in Figure 1B.

alkalinity determination, and while the other part is sealed and stored at a low temperature for onshore hydrocarbon determination.

The pore water headspace was injected into a gas chromatograph for methane concentration analysis (Agilent 6,850). The carrier gas was nitrogen at a flow rate of 20 ml/min. The precision of the methane analysis is ±3%.

## Results

### Geochemical constraints on the methane seep activity

In the shallow part, the methane concentration of pore water increased significantly with the increase in depth.

At a depth of 11.44 m below the seafloor, the methane concentration in the headspace of pore water showed a low characteristic of 0.002–0.11 mmol/L in borehole 18-01. Methane concentration rise sharply below 11.44 m, from 0.11 mmol/L at 11.44 m to 2.82 mmol/L (13.54 m). This result indicates that anaerobic oxidation and sulfate reduction of methane are strongly developed at a depth of 11.44 m. The findings reveal that the depth of the Sulfate-Methane Interface (SMI) is 11.44 mbsf. The high values of methane concentration (2.64 and 2.59 mmol/L, respectively) are observed at the depths of 32.08 m and 53.14 mbsf respectively (Figure 3A), indicating the possible migration and occurrence of high-concentration methane fluid in the original formation. In borehole 18-05, the variation in methane concentration in pore water is similar to that in borehole 18-01. The methane concentration remains low in characteristics in shallow depths of

0–1.04 m below the seafloor, while the methane concentration in the strata below 1.04 mbsf increases rapidly, implying that the depth of SMI is 1.04 m. However, at the depths of 5.94, 11.79, 43.42, and 47.79 m, methane concentrations all represented high concentration characteristics (Figure 3B) (Li, et al., 2020).

## Seismic chimneys

Methane fluid escapes from conduits can be recognized by seismic and sub-bottom profile data. Seismic chimneys are one of these features. They are vertical to sub-vertical seismic anomalies with circular or elliptical planforms that hydraulically connect deeper stratigraphic layers with the overburden (Karstens and Berndt, 2015). Within seismic chimney structures, seismic amplitude blanking and chaotic reflections are commonly observed (Callow, et al., 2021). Seismic chimneys have been observed extensively on the Western slope of the Okinawa Trough, and they may act as a pathway for methane fluids, allowing upward migration to the seafloor and eventually into the water column. Based on the seismic observations, we classified the seismic chimneys in the study area into four groups.

Type-A chimneys appear to be associated with seafloor domes or pockmarks. In the seismic profiles, the presence of chaotic or blanking reflections has been observed within type-A seismic chimneys. The surrounding reflections bend upwards with reduced amplitude at the lateral margin of chimneys. Type-A chimneys terminate close to the seafloor and are connected to domes or pockmarks. For example, the anomaly of Figure 4A narrows upwards and is terminated with a dome on the seafloor, whereas the chimney shown in Figure 4C is connected to a pockmark on the seafloor. The instantaneous frequency attribute
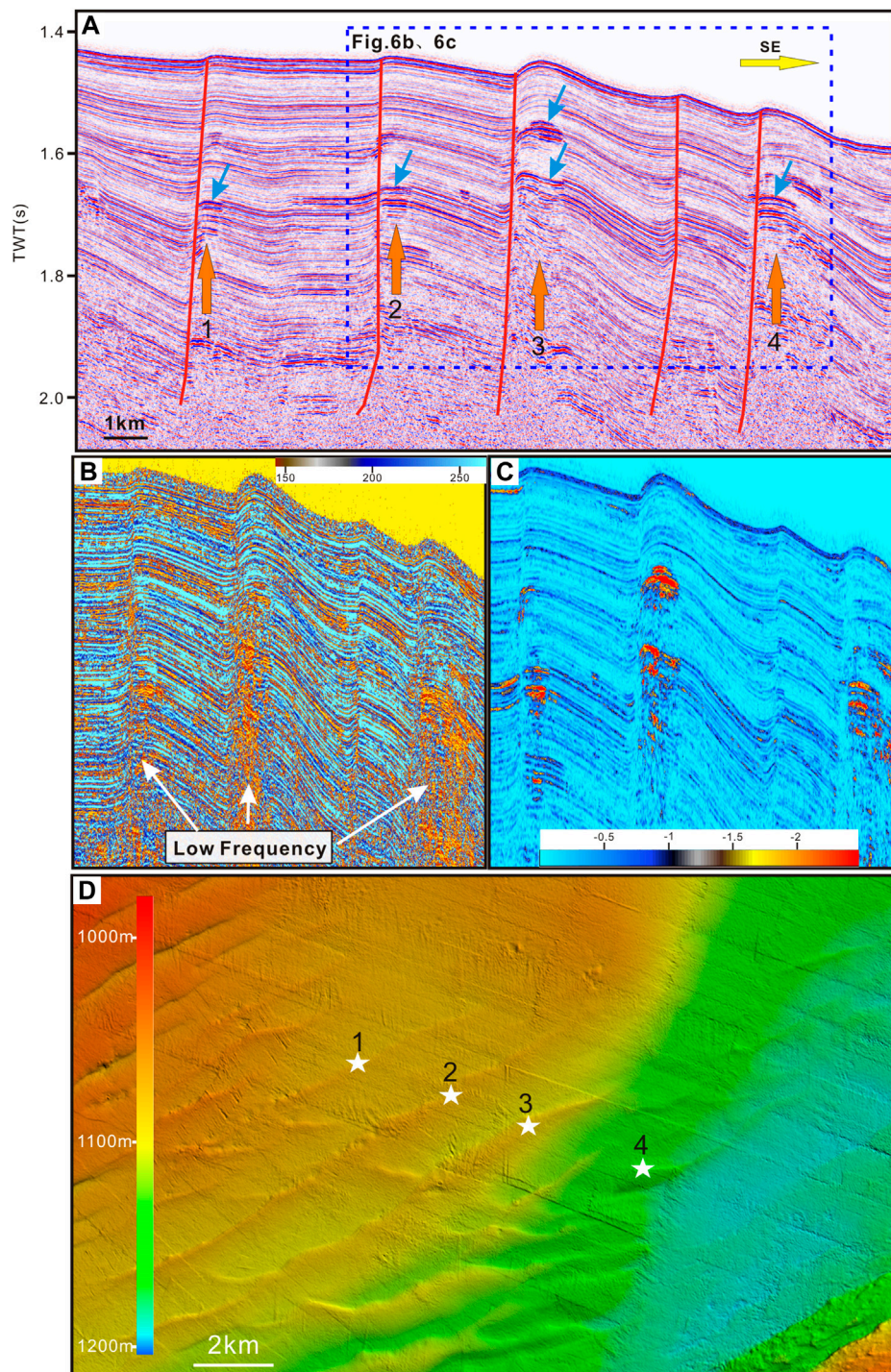
**FIGURE 6**
Type-C seismic chimneys. **(A)** The seismic profile shows type-C chimneys; **(B)** The Instantaneous frequency attribute profile; **(C)** The high-frequency attenuation attribute profile. The location of **(B)**; **(C)** is shown in Figure 6A. Low-frequency and high-frequency attenuation anomalies are all reveal the presence of fluids. **(D)** Multibeam bathymetry data reveal the relationship between chimneys and faults. White pentacles represent corresponding chimneys in Figure 6A. See locations in Figure 1B.
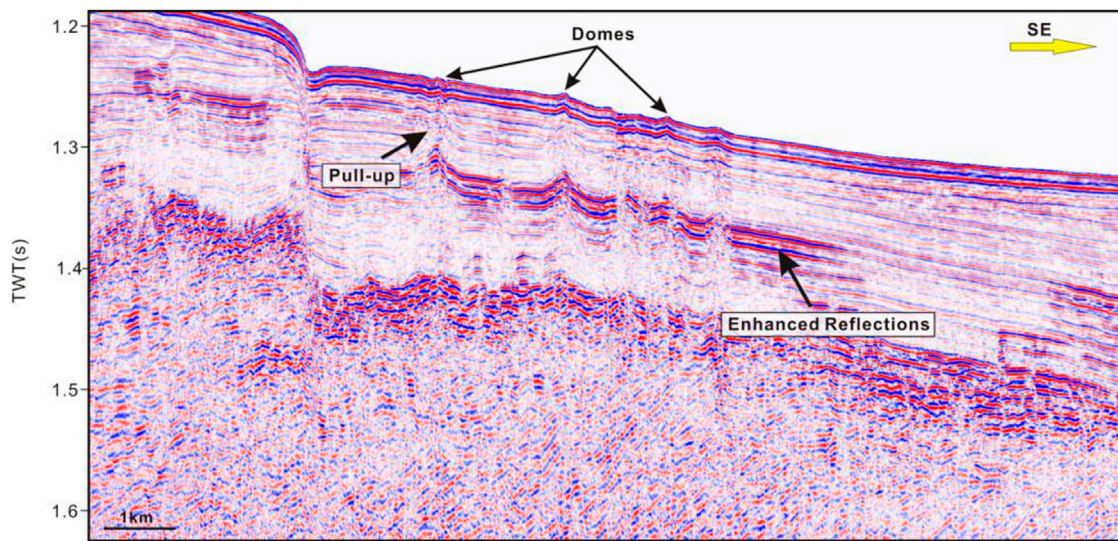
**FIGURE 7**
Seismic profile shows type-D seismic chimneys. This type of chimney is distinguished by elongated, adjacent to which several enhanced reflections have been observed. See locations in Figure 1B.

is probably the best for mapping frequency variation due to the presence of fluid in the shallow sediments. In the instantaneous frequency profiles (Figures 4B,D), the two chimneys depicted in Figure 4 all present low-frequency anomalies that differ from the surrounding area.

Type-B chimneys are vertically amplitude blanking or chaotic reflections with characteristics similar to type-A, but they do not extend to the seafloor. The majority of them are terminated by high amplitude patches or disturbed zones of comparable width to the underlying distorted zone (Figure 5).

Type-C seismic chimneys are appearing along the deep-seated faults. Reduced reflectivity or chaotic reflections occur within type-C chimneys, and several enhanced reflections or bright spots are sometimes observed within or immediately adjacent to them, like in Figure 6. Four chimneys with chaotic and enhanced reflections along faults are observed in Figure 6, and the distribution of enhanced reflections is limited to the local topographic heights of faults. The instantaneous frequency profile clearly shows low-frequency anomalies along faults, which are speculated to be caused by fluid flow. Due to energy dissipation, seismic waves pass through gas-bearing sedimentary, resulting in a relatively great attenuation effort, particularly for high-frequency signals. The seismic high-frequency attenuation attribute is frequently used to identify fluids by calculating the rate of seismic energy attenuation in the high-frequency band. Therefore, the high value observed in the high-frequency attenuation profile within chimneys suggests that the strata are fluid-rich. Above all, the faulting appears to have aided in

decreasing the top seal's integrity or creating a more efficient escape path for the fluids underneath.

Type-D chimneys have elongated, slightly meandering bands and are accompanied by bright spots or enhanced reflections; their seismic signature is similar to that of pipes. Type-D chimneys usually appear in groups, and some of them connect domes on the present-day seafloor (Figure 7).

## Seafloor domes

Submarine domes, which are thought to be a precursor of pockmark formation (Koch, et al., 2015), are the most widely observed evidence of potential methane fluid activity on the Western slope of the Okinawa Trough. Some submarine domes have been discovered in the study area (Figure 1). The majority of them are located in water depths ranging from 900 to 980 m. The height of the mud volcanoes ranges from less than 10 m to tens of meters above the seafloor. While the diameters at the base range between 100 and 600 m. The slope of the mud volcanoes varies between 1 and 16°.

The domes in the study area can be classified into three types based on their morphology using multibeam bathymetry. Type-A domes have flat edifices with gentle slopes on their crests, e.g., Figure 8A. The dome rises only about 2–4 m above the surrounding seabed, with slopesranging from 1° to 2°. The diameter of the dome is approximately 250 m. Type-B domes are relatively large and have a crater-like top with a complex, e.g., Figures 8B,C. The dome shown in Figure 8B has two crests: one main crest and the other crest. It rises 3–7 m above the surrounding seafloor and has a diameter of
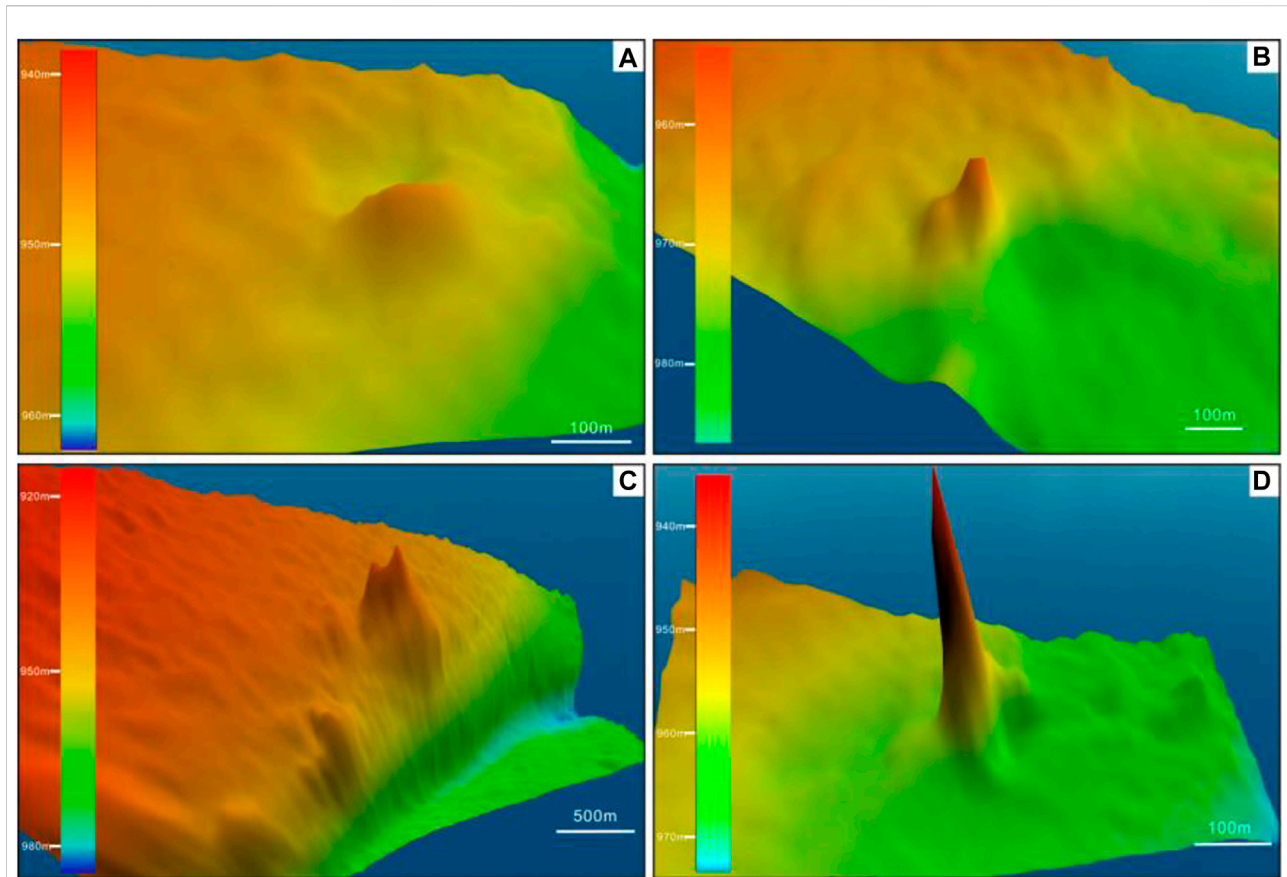
**FIGURE 8**
Multibeam data of domes. **(A)** An example of a type-A dome, which has flat edifices with gentle slopes on their crests; **(B)** and **(C)** Two examples of type-A domes, which have an irregular shape; **(D)** An example of a type-C dome, which are more conical with a relatively steep slope. See locations in Figure 1C.

about 250 m. The slope angle of type-B is larger than that of type-A, and the slope angle of Figure 8B is about 2°–5°. Figure 8C is the largest dome in the study area, and it also belongs to type-B. It has a more irregular shape. Each flank rises between 9 and 20 m above the seafloor and has a diameter ranging from 300 to 600 m. Type-C domes are more conical with relatively steep slopes. Figure 8D is an example of a type-C dome. The dome is 25 m tall with a 16-degree slope and a diameter of only 130 m. Multibeam bathymetry data reveals that several domes are surrounded by collapse subsidence structures in the study area. Some depressions are annular around the domes, as shown in Figures 9A,B, while the majority are on the side adjacent to the domes, such as Figures 9C,D. The depths of depressions are usually several meters below the seabed.

Sub-bottom profile and high-resolution seismic surveys were conducted in the study area, providing us with an excellent opportunity to better understand the internal characteristics of the submarine domes. Domes are cone-shaped, with internal seismic expressions of blanking or chaotic seismic facies. The majority of the domes in the study

area are linked to a seismic chimney, such as the domes shown in Figure 10. The chaotic or blanking reflections in the feeder channels and surrounding strata on both sides of domes exhibit systematically distorted reflectors like pull-up reflections. Parabolic-shaped anomalies in the water column have been observed above domes, whereas flares are also observed in the same place based on multibeam bathymetry. The dome is shown in seismic data (Figure 11) and also presents acoustic flares in multibeam bathymetry data.

## Pockmarks

Pockmarks, nearly circular depressions, are related to the escape of fluids and gases through the seafloor and are common on continental margins around the world (Cathles, et al., 2010; Dondurur, et al., 2011). Pockmarks are commonly located in areas where gas is present in near-surface sediments because of their association with the seepage of methane-rich fluids and
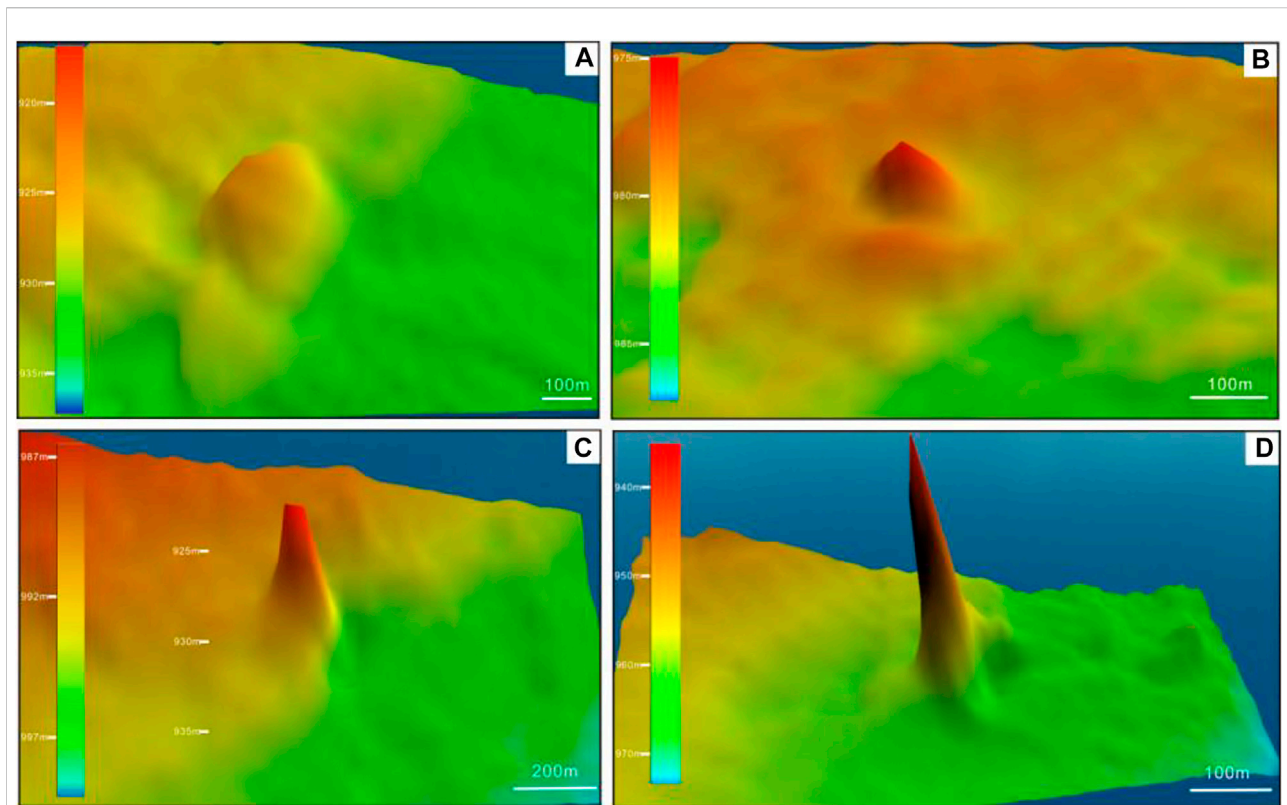
**FIGURE 9**
Mud volcanoes are surrounded by collapse subsidence structures. See locations in Figure 1C.

gases. Pockmarks form where fluids discharge rapidly enough through seafloor sediments to make them quick. As a result of focused fluid flow, seismic chimneys may, form beneath pockmarks representing feeding channels for the upward migrating fluids and gases (Petersen et al., 2010).

Several pockmarks connected to a chimney have been observed in the study area. Figure 12 depicts an example seismic profile for a pockmark. Below the pockmark, chaotic and push-down reflections have been observed, as well as enhanced reflections on both flanks. In general, there is common agreement in that these push-down reflections are partially explained as velocity effects caused by low-velocity material, such as the migration of fluids or free gas (Bünz et al., 2012).

## Bright spots and enhanced reflections

Bright spots and enhanced reflections observed on seismic profiles have been attributed to gas accumulations, which are crucial indicators of methane-related fluids. Bright spots or enhanced reflections in the study area have reversed polarity compared to the seafloor reflection, strongly increased

amplitudes compared to the background, and typically with sharp lateral terminations. These amplitude anomalies are commonly found within or surrounding seismic chimneys and the depths of these reflections are viable and do not appear to correlate with specific stratigraphic layers (Figure 4, Figure 5, Figure 6, Figure 7).

## Discussion

### Origin of methane

The shallow depth of the SMI suggests an extremely high methane seepage flux and active methane anaerobic oxidation processes in both sites. According to the variations features of methane concentration in the pore, the depths of SMI in sites 18-01 and 18-05 are 11.44 and 1.04 m, respectively, indicating high-flux methane fluid seepages. It also confirms that seepages are still active at both sites, as evidenced by gas flares observed in the multibeam data.

Geochemical analysis of pore water molecular ratios and isotopic compositions shows that C1/C2 vary from 960.53 to 1 120.75 in the core 18-01 and from 1 064.66 to 1 546.74 in the
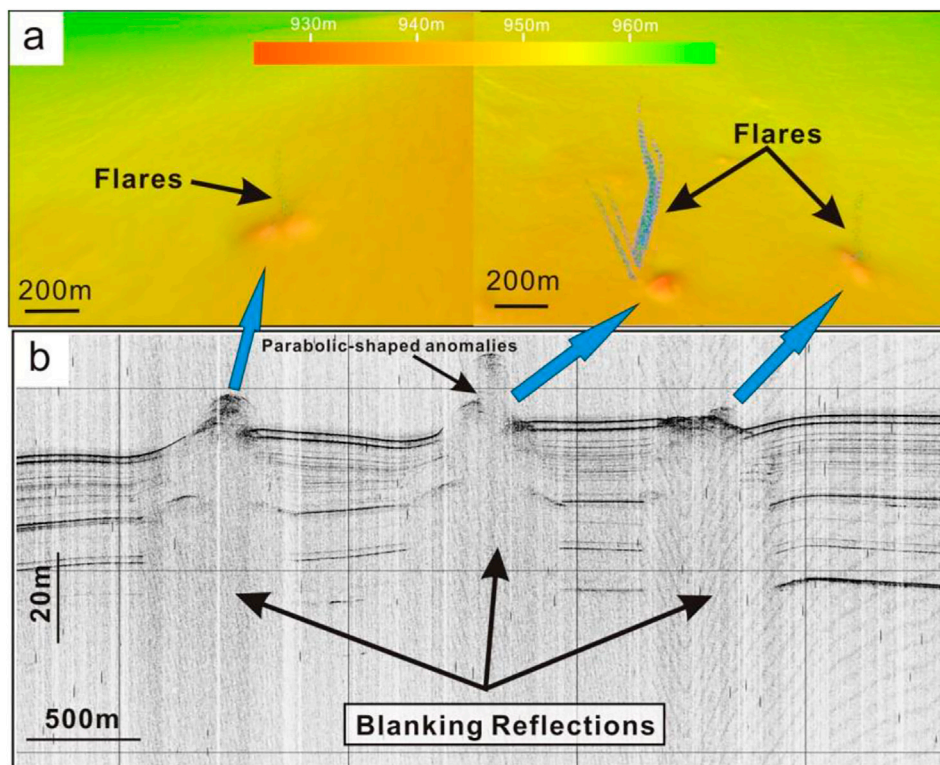
**FIGURE 10**
Multibeam and sub-bottom profile data show domes. **(A)** Bathymetry data show flares above domes. **(B)** The sub-bottom profile data show parabolic-shaped anomalies above domes. See locations in Figure 1C.

core 18-05, while the carbon isotopic values of pore water methane exhibit a variation from −36.07‰ to −56.60‰ V-PDB in the core 18-01 and from −36.10‰ to −62.92‰ V-PDB in the core 18-05 respectively. We concluded that the pore water methane is derived from a mixture of thermogenic and biogenic sources, primarily thermogenic, based on molecular ratios, stable carbon, and hydrogen isotopic compositions (Li, et al., 2020).

## Relationships between observed geophysical anomalies and methane seepages

Seismic chimneys are usually interpreted as focused fluid flow structures that hydraulically connect deeper stratigraphic layers with the overburden. Their formation is believed to be governed by overpressure-induced hydrofracturing of an impermeable cap rock (Karstens and Berndt, 2015).

When methane-rich fluids pass through sediments, the primary sedimentary structures may be physically altered, resulting in the formation of new sediments and structures.

Fluid flow reaching the seafloor can cause seabed expressions such as domes and pockmarks. In the study area, domes and pockmarks are frequently found above seismic chimneys, indicating that fluid migration plays an important role in their formation. Chimneys that reach the seafloor forming pockmarks likely indicate recent or active fluid venting (Horozal et al., 2017). Fluids are initially trapped beneath fine-grained sediments, which form a capillary seal, and when they accumulate to a certain thickness, the seal fails, releasing fluids into a chimney, where water is displaced as the chimney moves upward. Then, the surface begins to deform, and the first pockmarks appear when the chimney reaches about halfway to the seafloor. Following that, sediment deformation above the chimney worsen, and pockmarks become more common. The pockmarks merge into a large pockmark with dimensions similar to the chimney. The gas pocket quickly drains when the chimney reaches the surface. Capillary forces draw the water back into the fine layers of the failed portion of the seal by capillary forces, and it is healed. Fluids accumulate beneath it once more, and the chimney formation process may repeat itself if the fluid again accumulates to a thickness (Cathles, et al., 2010). However, Seafloor doming may indicate the early stages of fluid discharge (Horozal, et al., 2017). Accumulation of gaseous
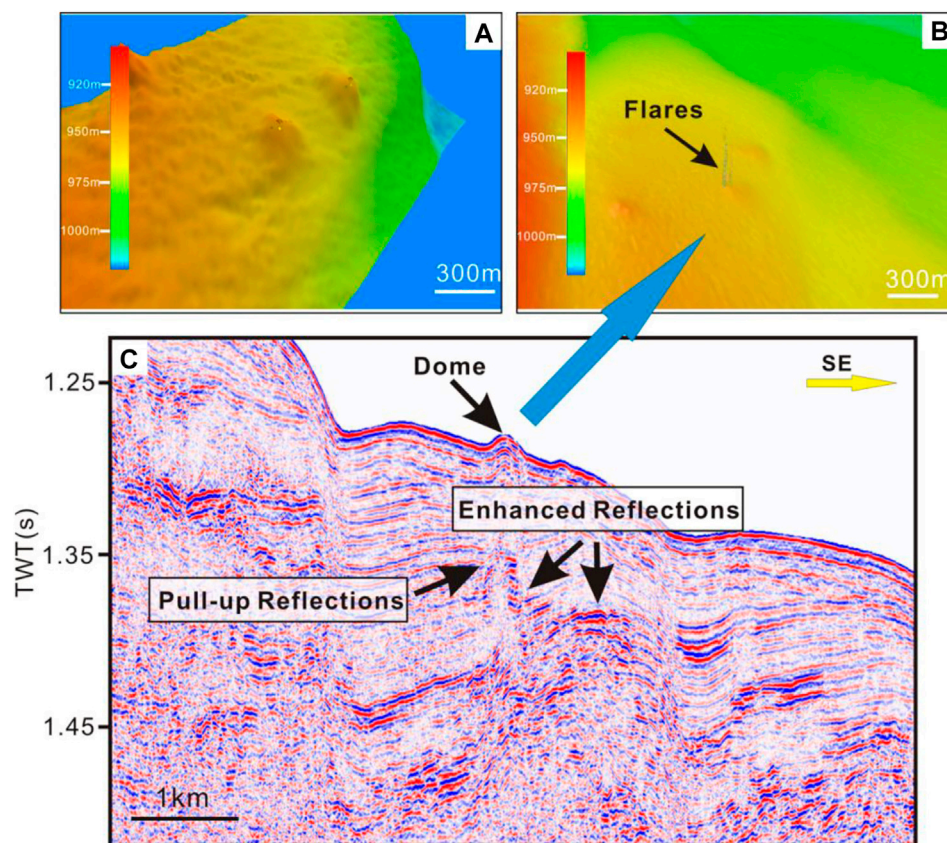
**FIGURE 11**
Multibeam data and seismic profile show a dome. **(A)** and **(B)** Bathymetry data show flare above the dome. **(C)** The seismic profile data of the dome. Several amplitude anomalies such as pull-up reflections and enhanced reflections were observed around the feeder zone of the dome. See locations in Figure 1C.

methane can generate seabed domes in soft cohesive sediments. The sediment may deform to accommodate the gas as a mechanical response to the increasing accumulation of fluids. Rising pressures from the accumulating fluids produce an upward force, which causes sediment doming (Roy et al., 2019). On the other hand, not all the chimneys extend to the seafloor, forming seafloor expressions, which may indicate that the venting is gradual and focused (Hillman et al., 2018).

In the study area, the multibeam echosounder and sub-bottom profile data have revealed several chimneys that reach the seafloor and form domes or pockmarks linked to flares, indicating that there is active upward migration of fluids occurring (Hillman, et al., 2018). However, there are also domes or pockmarks on the seafloor that are not associated with flares. The absence of flares may suggest that certain seep locations are currently inactive or are not releasing enough fluids, causing an anomaly in the water column (Roy, et al., 2019).

The enhanced reflections and bright spots could be caused by a variety of factors, including variations in lithology and the presence of authigenic carbonate deposits. The presence of free gas in the sediment pore space is another important explanation for enhanced reflections. The presence of free gas can induce p-wave velocity and a increase impedance contrast. This gives rise to an abnormally high amplitude from the top of the free gas zone. We suspect that the enhanced reflections are caused by the local accumulation of free gas within sediments due to their proximity to seismic chimneys.

## Possible triggered factors of methane seepages

Multibeam bathymetric data shows that most methane seepages are discovered along steep bathymetric slopes or faults, indicating that the tectonic setting is an important factor triggering the methane seepages. The Okinawa Trough is a back-arc basin formed by extension within the continental lithosphere behind the Ryukyu trench-arc system. Regional extension weakens the overburden, which may result in a
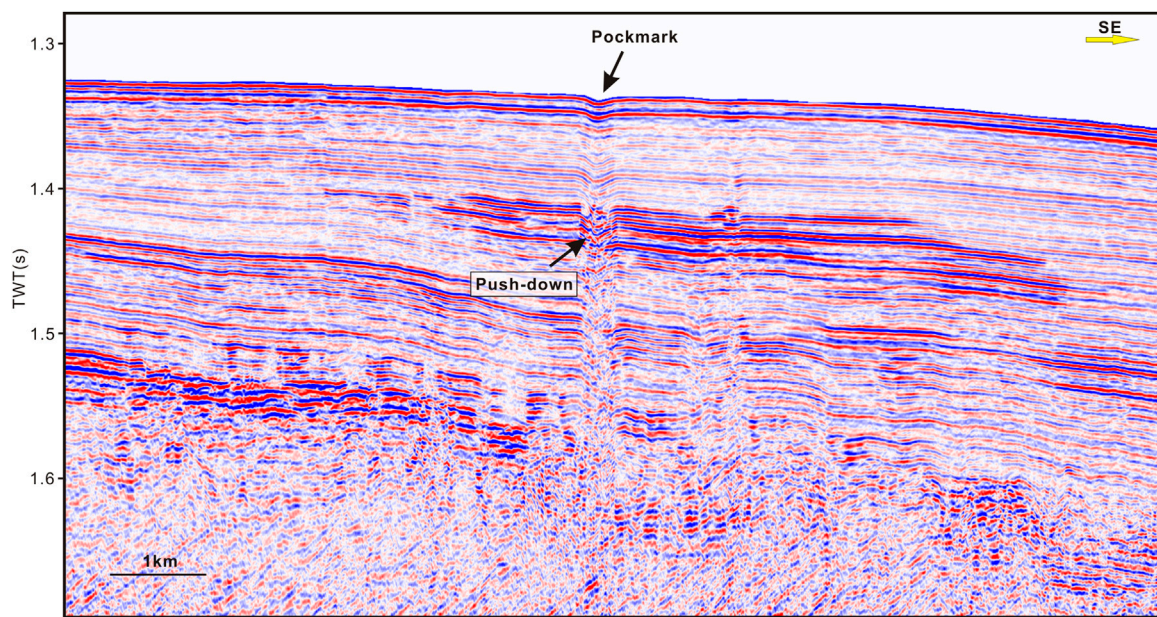
**FIGURE 12**
Seismic data show a pockmark associated with a seismic chimney. The presence of chaotic and push-down reflections has been observed below the pockmark, and enhanced reflections have been observed on both flanks. See locations in Figure 1C.

local decrease in the tensile strength of the cap rock, thereby reducing its resistance to hydrofracturing. Most chimneys and domes are distrubuted along the steep bathymetric slopes or faults that reveal the relationship. Based on the seismic profiles, numerous high-angle normal faults have developed in the study area. The orientation of these faults is roughly parallel to the great axis of the Okinawa Trough. In the study area, most seeps are associated with faults. Some of them are observed near faults, like Figure 7, Figure 11. Several blanking or chaotic reflections have been observed along faults, as well as enhanced reflections or bright spots that are commonly limited to local topographic heights of faults, like in Figure 6, indicating that faults may play an important role in fluid migration and accumulation.

Not all methane seepages are associated with faults. Several seepages in the study area do not exhibit a clear relationship with faults, as in Figure 12. Besides the tectonic setting, overpressure and rapid sedimentation are also important triggering factors of methane seepages. When the pore-fluid overpressure exceeds the internal forces or lithostatic pressure, vertical hydraulic fracturing may occur (Dimitrov, 2002). Overpressured sediments must be initially isolated by impermeable barriers. Such conduits form the opening of the impermeable barriers and provide a pathway for methane migration from the source. Overpressure generation is likely to be complicated and influenced by many factors (Lei et al., 2011). A rapid sedimentation rate is the main reason for overpressure in sedimentary layers (Milkov, 2000; Dimitrov, 2002; Talukder et al., 2008). The Okinawa Trough deposited a thick Pliocene-

Quaternary sedimentary layer, up to thousands of meters. The sedimentary rate is much higher than in the oceans, especially on the Western slope, which could be up to 10–40 cm/ka. During glacial periods, the drop in sea-level caused the continental shelf to narrow. The YangtzeRiver transports a large amount of terrigenous source debris materials directly to the continental slope, where it is rapidly deposited near the Western slope of the Okinawa Trough (Berné et al., 2002). When overburden loads increase dramatically due to high sedimentation, pore fluids cannot be expelled leading to a reduction in pore volume that cannot be balanced. Then, pore fluid will bear part of the load pressure leading to hydrodynamic pressure being higher than the hydrostatic pressure, then producing the overpressure (Talukder et al., 2007).

## Conclusion

Pore water geochemical analysis of seabed drilling indicated an extremely high methane seepage flux and active methane anaerobic oxidation processes on the Western slope of the Okinawa Trough. At the same time, numerous methane seepage-related features, such as seismic chimneys, pockmarks, submarine domes, and bright spots or enhanced reflection, have been observed in geophysics data near the drilling sites. These geophysical features are associated with each other. Chaotic or blanking reflections have been observed within seismic chimneys, and several enhanced reflections or bright spots are sometimes observed within or immediately adjacent to them.

Pockmarks and domes are often connected to seismic chimneys, indicating that fluid migration plays an important role in their formation. The different geophysical features may represent different stages of methane seepage. Fluid quickly drains, causing severe sediment deformation and forming pockmarks, whereas domes may be an indication of the early stages of fluid discharge. Chimneys that do not extend to the seafloor may indicate that the venting is gradual and focused. Flares linked to domes or pockmarks may indicate that the fluid migration is active.

Tectonic setting, overpressure, and rapid sedimentation all triggered the existence of methane seepages on the Western slope of the Okinawa Trough. Most chimneys and domes are distributed along the steep bathymetric slopes or faults, revealing that tectonic activity plays an important role in the methane seepages. Besides that, overpressure and rapid sedimentation are important triggering factors of methane seepages which do not exhibit a clear relationship with faults.

## Data availability statement

The original contributions presented in the study are included in the article/supplementary material, further inquiries can be directed to the corresponding author.

## Author contributions

DL performed the data analyses and wrote the manuscript. FC contributed to the conception of the study; QL contributed to the geochemical analysis of pore water.

GY, YS, and GD contributed to acquiring the data used in the study. AL contributed to interpreting the multi-beam bathymetric data.

## Funding

## Conflict of interest

The authors declare that the research was conducted in the absence of any commercial or financial relationships that could be construed as a potential conflict of interest.

## Publisher's note

All claims expressed in this article are solely those of the authors and do not necessarily represent those of their affiliated organizations, or those of the publisher, the editors and the reviewers. Any product that may be evaluated in this article, or claim that may be made by its manufacturer, is not guaranteed or endorsed by the publisher.

## References

Benjamin, U. K., and Huuse, M. (2017). Seafloor and buried mounds on the Western slope of the Niger Delta. *Mar. Petroleum Geol.* 83, 158–173. doi:10.1016/j.marpetgeo.2017.02.023

Berndt, C., Feseker, T., Treude, T., Krastel, S., Liebetrau, V., Niemann, H., et al. (2014). Temporal constraints on hydrate-controlled methane seepage off svalbard. *Science* 343 (6168), 284–287. doi:10.1126/science.1246298

Berné, S., Vagner, P., Guichard, F., Lericolais, G., Liu, Z., Trentesaux, A., et al. (2002). Pleistocene forced regressions and tidal sand ridges in the East China Sea. *Mar. Geol.* 188 (3), 293–315. doi:10.1016/s0025-3227(02)00446-2

Bünz, S., Polyanov, S., Vadakkepuliyambatta, S., Consolaro, C., and Mienert, J. (2012). Active gas venting through hydrate-bearing sediments on the Vestnesa Ridge, offshore W-Svalbard. *Mar. Geol.* 332–334 (0), 189–197. doi:10.1016/j.margeo.2012.09.012

Callow, B., Bull, J. M., Provenzano, G., Bottner, C., Birinci, H., Robinson, A. H., et al. (2021). Seismic chimney characterisation in the North Sea – implications for pockmark formation and shallow gas migration. *Mar. Petroleum Geol.* 133, 105301. doi:10.1016/j.marpetgeo.2021.105301

Cathles, L. M., Su, Z., and Chen, D. (2010). The physics of gas chimney and pockmark formation, with implications for assessment of seafloor hazards and gas sequestration. *Mar. Petroleum Geol.* 27 (1), 82–91. doi:10.1016/j.marpetgeo.2009.09.010

Chen, L., Chiang, H-T., Wu, J-N., Chiao, L. Y., Shyu, C. T., Liu, C. S., et al. (2020). The focus thermal study around the spreading center of southwestern Okinawa trough. *Tectonophysics* 796, 228649. doi:10.1016/j.tecto.2020.228649

Chun, J-H., Ryu, B-J., Son, B-K., Kim, J. H., Lee, J. Y., Bahk, J. J., et al. (2011). Sediment mounds and other sedimentary features related to hydrate occurrences in a columnar seismic blanking zone of the Ulleung Basin, East Sea, Korea. *Mar. Petroleum Geol.* 28 (10), 1787–1800. doi:10.1016/j.marpetgeo.2011.06.006

Crutchley, G. J., Berndt, C., Geiger, S., Klaeschen, D., Papenberg, C., Klaucke, I., et al. (2013). Drivers of focused fluid flow and methane seepage at south Hydrate Ridge, offshore Oregon, USA. *Geology* 41 (5), 551–554. doi:10.1130/g34057.1

Dewangan, P., Sriram, G., Kumar, A., Mazumdar, A., Peketi, A., Mahale, V., et al. (2021). Widespread occurrence of methane seeps in deep-water regions of Krishna-Godavari basin, Bay of Bengal. *Mar. Petroleum Geol.* 124, 104783. doi:10.1016/j.marpetgeo.2020.104783

Dimitrov, L. I. (2002). Mud volcanoes—The most important pathway for degassing deeply buried sediments. *Earth-Science Rev.* 59 (1), 49–76. doi:10.1016/s0012-8252(02)00069-7

Dixit, A., and Mandal, A. (2020). Detection of gas chimney and its linkage with deep-seated reservoir in poseidon, NW shelf, Australia from 3D seismic data using multi-attribute analysis and artificial neural network approach. *J. Nat. Gas Sci. Eng.* 83, 103586. doi:10.1016/j.jngse.2020.103586

Dondurur, D., Çifçi, G., Drahor, M. G., and Coskun, S. (2011). Acoustic evidence of shallow gas accumulations and active pockmarks in the İzmir Gulf, Aegean sea. *Mar. Petroleum Geol.* 28 (8), 1505–1516. doi:10.1016/j.marpetgeo.2011.05.001

Graves, C. A., James, R. H., Sapart, C. J., Stott, A. W., Wright, I. C., Berndt, C., et al. (2017). Methane in shallow subsurface sediments at the landward limit of the gas hydrate stability zone offshore Western Svalbard. *Geochimica Cosmochimica Acta* 198, 419–438. doi:10.1016/j.gca.2016.11.015

Guan, H., Liu, L., Hu, Y., Li, S., Li, N., Sun, Z., et al. (2022). Rising bottom-water temperatures induced methane release during the middle Holocene in the Okinawa Trough, East China Sea. *Chem. Geol.* 590, 120707. doi:10.1016/j.chemgeo.2022.120707

Guan, H., Sun, Z., Mao, S., Xu, L., Cao, H., Geng, W., et al. (2019). Authigenic carbonate formation revealed by lipid biomarker inventory at hydrocarbon seeps: A case study from the Okinawa Trough. *Mar. Petroleum Geol.* 101, 502–511. doi:10.1016/j.marpetgeo.2018.12.028

Gullapalli, S., Dewangan, P., Kumar, A., Dakara, G., and Mishra, C. (2019). Seismic evidence of free gas migration through the gas hydrate stability zone (GHSZ) and active methane seep in Krishna-Godavari offshore basin. *Mar. Petroleum Geol.* 110, 695–705. doi:10.1016/j.marpetgeo.2019.07.052

He, J. X., Wang, S. H., Zhang, W., Yan, W., and Lu, Z. (2016). Characteristics of mud diapirs and mud volcanoes and their relationship to oil and gas migration and accumulation in a marginal basin of the northern South China Sea. *Environ. Earth Sci.* 75 (15), 1122. doi:10.1007/s12665-016-5894-9

Hillman, J. I. T., Crutchley, G. J., and Kroeger, K. F. (2020). Investigating the role of faults in fluid migration and gas hydrate formation along the southern Hikurangi Margin, New Zealand. *Mar. Geophys. Res.* 41 (1), 8. doi:10.1007/s11001-020-09400-2

Hillman, J. I. T., Klaucke, I., Bialas, J., Feldman, H., Drexler, T., Awwiller, D., et al. (2018). Gas migration pathways and slope failures in the danube fan, Black Sea. *Mar. Petroleum Geol.* 92, 1069–1084. doi:10.1016/j.marpetgeo.2018.03.025

Horozal, S., Bahk, J. J., Urgeles, R., Kim, G. Y., Cukur, D., Kim, S. P., et al. (2017). Mapping gas hydrate and fluid flow indicators and modeling gas hydrate stability zone (GHSZ) in the Ulleung Basin, East (Japan) Sea: Potential linkage between the occurrence of mass failures and gas hydrate dissociation. *Mar. Petroleum Geol.* 80, 171–191. doi:10.1016/j.marpetgeo.2016.12.001

Karstens, J., and Berndt, C. (2015). Seismic chimneys in the Southern Viking Graben – implications for palaeo fluid migration and overpressure evolution. *Earth Planet. Sci. Lett.* 412 (0), 88–100. doi:10.1016/j.epsl.2014.12.017

Kempka, T., Unger, V., and Kühn, M. (2016). Seismic chimney formation induced by upward-migrating methane in the nordland group, southern viking graben. *Energy Procedia* 97, 427–432. doi:10.1016/j.egypro.2016.10.040

Koch, S., Berndt, C., Bialas, J., Haeckel, M., Crutchley, G., Papenberg, C., et al. (2015). Gas-controlled seafloor doming. *Geology* 43 (7), 571–574. doi:10.1130/g36596.1

Krabbenhoeft, A., Bialas, J., Klaucke, I., Crutchley, G., Papenberg, C., and Netzeband, G. L. (2013). Patterns of subsurface fluid-flow at cold seeps: The Hikurangi Margin, offshore New Zealand. *Mar. Petroleum Geol.* 39 (1), 59–73. doi:10.1016/j.marpetgeo.2012.09.008

Lei, C., Ren, J., Clift, P. D., Wang, Z., Li, X., and Tong, C. (2011). The structure and formation of diapirs in the yinggehai–song hong basin, south China sea. *Mar. Petroleum Geol.* 28 (5), 980–991. doi:10.1016/j.marpetgeo.2011.01.001

Li, A., Cai, F., Wu, N., Li, Q., Yan, G., Sun, Y., et al. (2021). Structural controls on widespread methane seeps in the back-arc basin of the Mid-Okinawa Trough. *Ore Geol. Rev.* 129, 103950. doi:10.1016/j.oregeorev.2020.103950

Li, Q., Cai, F., Liang, J., Shao, H., Dong, G., Wang, F., et al. (2015). Geochemical constraints on the methane seep activity in Western slope of the middle Okinawa Trough, the East China Sea. *Sci. China Earth Sci.* 58, 986–995. doi:10.1007/s11430-014-5034-x

Li, Q., Cai, F., Yan, G., Sun, Y., Li, A., Liu, D., et al. (2020). Origin of pore water methane recovered from mud volcanos in the Okinawa Trough. *Mar. Geol. Front.* 36 (9), 79–86. doi:10.16028/j.1009-2722.2020.062

Logan, G. A., Jones, A. T., Kennard, J. M., Ryan, G. J., and Rollet, N. (2010). Australian offshore natural hydrocarbon seepage studies, a review and re-evaluation. *Mar. Petroleum Geol.* 27 (1), 26–45. doi:10.1016/j.marpetgeo.2009.07.002

Luo, D., Cai, F., and Wu, Z. (2017). Numerical simulation for accuracy of velocity analysis in small-scale high-resolution marine multichannel seismic technology. *J. Ocean. Univ. China* 16 (3), 370–382. doi:10.1007/s11802-017-3145-7

Luo, D., Cai, F., Wu, Z., Yan, G., and Du, R. (2019). The key technologies of marine small scale high resolution multichannel seismic high-precision imaging. *Chin. J. Geophys.* 62 (2), 730–742. (in Chinese). doi:10.6038/cjg2019M0178

Magalhaes, V. H., Buffett, B., Archer, D., McGuire, P. C., Pinheiro, L. M., and Gardner, J. M. (2019). Effects of oceanographic changes on controlling the stability of gas hydrates and the formation of authigenic carbonates at mud volcanoes and seepage sites on the Iberian margin of the Gulf of Cadiz. *Mar. Geol.* 412, 69–80. doi:10.1016/j.margeo.2019.03.002

Milkov, A. V. (2000). Worldwide distribution of submarine mud volcanoes and associated gas hydrates. *Mar. Geol.* 167 (1–2), 29–42. doi:10.1016/s0025-3227(00)00022-0

Miller, P., Dasgupta, S., and Shelander, D. (2012). Seismic imaging of migration pathways by advanced attribute analysis, Alaminos Canyon 21, Gulf of Mexico. *Mar. Petroleum Geol.* 34 (1), 111–118. doi:10.1016/j.marpetgeo.2011.09.005

Minami, H., Okada, C., Saito, K., and Ohara, Y. (2022). Evidence of an active rift zone in the northern Okinawa Trough. *Mar. Geol.* 443, 106666. doi:10.1016/j.margeo.2021.106666

Mohammedyasin, S. M., Lippard, S. J., Omosanya, K. O., Johansen, S., and Harishidayat, D. (2016). Deep-seated faults and hydrocarbon leakage in the snøhvit gas field, hammerfest basin, southwestern barents sea. *Mar. Petroleum Geol.* 77, 160–178. doi:10.1016/j.marpetgeo.2016.06.011

Netzeband, G. L., Krabbenhoeft, A., Zillmer, M., Petersen, C., Papenberg, C., and Bialas, J. (2010). The structures beneath submarine methane seeps: Seismic evidence from Opouawe Bank, Hikurangi Margin, New Zealand. *Mar. Geol.* 272 (1–4), 59–70. doi:10.1016/j.margeo.2009.07.005

Ning, X., Shiguo, W., Buqing, S., Bing, L., Liangqing, X., Xiujuan, W., et al. (2009). Gas hydrate associated with mud diapirs in southern Okinawa Trough. *Mar. Petroleum Geol.* 26 (8), 1413–1418. doi:10.1016/j.marpetgeo.2008.10.001

Palomino, D., López-González, N., Vázquez, J-T., Fernandez-Salas, L. M., Rueda, J. L., Sanchez-Leal, R., et al. (2016). Multidisciplinary study of mud volcanoes and diapirs and their relationship to seepages and bottom currents in the Gulf of Cádiz continental slope (northeastern sector). *Mar. Geol.* 378, 196–212. doi:10.1016/j.margeo.2015.10.001

Park, J-O., Tokuyama, H., Shinohara, M., Suyehiro, K., and Taira, A. (1998). Seismic record of tectonic evolution and backarc rifting in the southern Ryukyu island arc system. *Tectonophysics* 294 (1), 21–42. doi:10.1016/s0040-1951(98)00150-4

Paull, C. K., Hecker, B., Commeau, R., Freeman-Lynde, R. P., Neumann, C., Corso, W. P., et al. (1984). Biological communities at the Florida escarpment resemble hydrothermal vent taxa. *Science* 226 (4677), 965–967. doi:10.1126/science.226.4677.965

Petersen, C. J., Bünz, S., Hustoft, S., Mienert, J., and Klaeschen, D. (2010). High-resolution P-Cable 3D seismic imaging of gas chimney structures in gas hydrated sediments at an Arctic sediment drift. *Mar. Petroleum Geol.* 27 (9), 1981–1994. doi:10.1016/j.marpetgeo.2010.06.006

Rovere, M., Gamberi, F., Mercorella, A., Rashed, H., Gallerani, A., Leidi, E., et al. (2014). Venting and seepage systems associated with mud volcanoes and mud diapirs in the southern Tyrrhenian Sea. *Mar. Geol.* 347, 153–171. doi:10.1016/j.margeo.2013.11.013

Roy, S., Senger, K., Hovland, M., Romer, M., and Braathen, A. (2019). Geological controls on shallow gas distribution and seafloor seepage in an Arctic fjord of Spitsbergen, Norway. *Mar. Petroleum Geol.* 107, 237–254. doi:10.1016/j.marpetgeo.2019.05.021

Schwalenberg, K., Haeckel, M., Poort, J., and Jegen, M. (2010). Evaluation of gas hydrate deposits in an active seep area using marine controlled source electromagnetics: Results from Opouawe Bank, Hikurangi Margin, New Zealand. *Mar. Geol.* 272 (1–4), 79–88. doi:10.1016/j.margeo.2009.07.006

Shinjo, R., and Kato, Y. (2000). Geochemical constraints on the origin of bimodal magmatism at the Okinawa Trough, an incipient back-arc basin. *Lithos* 54 (3–4), 117–137. doi:10.1016/s0024-4937(00)00034-7

Shnyukov, E. F. (2013). Mud volcanoes of the Black Sea as a prospecting indicator of methane gas hydrates. *Lithol. Min. Resour.* 48 (2), 114–121. doi:10.1134/s0024490213010045

Sibuet, J. C., Deffontaines, B., Hsu, S. K., Thareau, N., Le Formal, J. P., and Liu, C. S. (1998). Okinawa trough backarc basin: Early tectonic and magmatic evolution. *J. Geophys. Res.* 103 (B12), 30245–30267. doi:10.1029/98jb01823

Sibuet, J-C., Letouzey, J., Barbier, F., Charvet, J., Foucher, J. P., Hilde, T. W. C., et al. (1987). Back arc extension in the Okinawa Trough. *J. Geophys. Res.* 92 (B13), 14041–14063. doi:10.1029/jb092ib13p14041

Somoza, L., León, R., Medialdea, T., Perez, L. F., Gonzalez, F. J., and Maldonado, A. (2014). Seafloor mounds, craters and depressions linked to seismic chimneys breaching fossilized diagenetic bottom simulating reflectors in the central and southern Scotia Sea, Antarctica. *Glob. Planet. Change* 123 (0), 359–373. Part B. doi:10.1016/j.gloplacha.2014.08.004

Suess, E. (2014). Marine cold seeps and their manifestations: Geological control, biogeochemical criteria and environmental conditions. *Int. J. Earth Sci.* 103 (7), 1889–1916. doi:10.1007/s00531-014-1010-0

Sun, Z., Wei, H., Zhang, X., Shang, L., Yin, X., Sun, Y., et al. (2015). A unique Fe-rich carbonate chimney associated with cold seeps in the Northern Okinawa Trough, East China Sea. *Deep Sea Res. Part I Oceanogr. Res. Pap.* 95 (0), 37–53. doi:10.1016/j.dsr.2014.10.005

Talukder, A. R., Bialas, J., Klaeschen, D., Brueckmann, W., Reston, T., and Petersen, J. (2008). Tectonic framework of the mud mounds, associated BSRs and submarine landslides, offshore Nicaragua Pacific margin. *J. Geol. Soc. Lond.* 165, 167–176. doi:10.1144/0016-76492007-012

Talukder, A. R., Bialas, J., Klaeschen, D., Buerk, D., Brueckmann, W., Reston, T., et al. (2007). High-resolution, deep tow, multichannel seismic and sidescan sonar survey of the submarine mounds and associated BSR off Nicaragua Pacific margin. *Mar. Geol.* 241 (1–4), 33–43. doi:10.1016/j.margeo.2007.03.002

Tsai, C-H., Hsu, S-K., Chen, S-C., Wang, S. Y., Lin, L. K., Huang, P. C., et al. (2021). Active tectonics and volcanism in the southernmost Okinawa Trough back-arc basin derived from deep-towed sonar surveys. *Tectonophysics* 817, 229047. doi:10.1016/j.tecto.2021.229047

Tsunogai, U., Maegawa, K., Sato, S., Komatsu, D. D., Nakagawa, F., Toki, T., et al. (2012). Coseimic massive methane release from a submarine mud volcano. *Earth Planet. Sci. Lett.* 341-344, 79–85. doi:10.1016/j.epsl.2012.06.004

Van Rensbergen, P., De Batist, M., Klerkx, J., Hus, R., Poort, J., Vanneste, M., et al. (2002). Sublacustrine mud volcanoes and methane seeps caused by dissociation of gas hydrates in Lake Baikal. *Geol.* 30 (7), 631–634. doi:10.1130/0091-7613(2002)030<0631:smvams>2.0.co;2

Wan, Z., Xu, X., Wang, X., Xia, B., and Sun, Y. (2017). Geothermal analysis of boreholes in the Shenhu gas hydrate drilling area, northern South China Sea: Influence of mud diapirs on hydrate occurrence. *J. Petroleum Sci. Eng.* 158, 424–432. doi:10.1016/j.petrol.2017.08.053

Wang, M., Li, Q., Cai, F., Liang, J., Yan, G., Wang, Z., et al. (2019). Formation of authigenic carbonates at a methane seep site in the middle Okinawa Trough, East China Sea. *J. Asian Earth Sci.* 185, 104028. doi:10.1016/j.jseaes.2019.104028

Wang, X., Liu, B., Qian, J., Zhang, X., Guo, Y., Su, P., et al. (2018). Geophysical evidence for gas hydrate accumulation related to methane seepage in the Taixinan Basin, South China Sea. *J. Asian Earth Sci.* 168, 27–37. doi:10.1016/j.jseaes.2017.11.011

Wei, J., Wu, T., Deng, X., Haider, S. W., Kahkashan, S., and Yang, S. (2021). Seafloor methane emission on the Makran continental margin. *Sci. Total Environ.* 801, 149772. doi:10.1016/j.scitotenv.2021.149772

Wenau, S., Spiess, V., Pape, T., and Fekete, N. (2015). Cold seeps at the salt front in the Lower Congo Basin I: Current methane accumulation and active seepage. *Mar. Petroleum Geol.* 67, 894–908. doi:10.1016/j.marpetgeo.2014.07.032

Williscroft, K., Grasby, S. E., Beauchamp, B., Little, C. T., Dewing, K., Birgel, D., et al. (2017). Extensive early cretaceous (albian) methane seepage on ellef ringnes island, Canadian high arctic. *Geol. Soc. Am. Bull.* 129 (7), 788–805. doi:10.1130/b31601.1

Xing, J., Jiang, X., and Li, D. (2016). Seismic study of the mud diapir structures in the Okinawa Trough. *Geol. J.* 51, 203–208. doi:10.1002/gj.2824

Xu, C., Wu, N., Sun, Z., Zhang, X., Geng, W., Cao, H., et al. (2021). Assessing methane cycling in the seep sediments of the mid-Okinawa Trough: Insights from pore-water geochemistry and numerical modeling. *Ore Geol. Rev.* 129, 103909. doi:10.1016/j.oregeorev.2020.103909

Xu, C., Wu, N., Sun, Z., Zhang, X., Geng, W., Cao, H., et al. (2018). Methane seepage inferred from pore water geochemistry in shallow sediments in the Western slope of the Mid-Okinawa Trough. *Mar. Petroleum Geol.* 98, 306–315. doi:10.1016/j.marpetgeo.2018.08.021

Yin, P., Berné, S., Vagner, P., Loubrieu, B., and Liu, Z. (2003). Mud volcanoes at the shelf margin of the East China Sea. *Mar. Geol.* 194 (3–4), 135–149. doi:10.1016/s0025-3227(02)00678-3